JOURNAL OF SOLID STATE CHEMISTRY 92, 1–7 (1991)

A Synchrotron Single Crystal X-Ray Structure Determination of a Small Crystal: Mo–Mo Double Bonds in the 3-D Microporous Molybdenum Phosphate $NH_4[Mo_2P_2O_{10}] \cdot H_2O$

H. E. KING, JR., LINDA A. MUNDI, KARL G. STROHMAIER, AND ROBERT C. HAUSHALTER*

Exxon Research and Engineering Co. Annandale, New Jersey 08801

Received September 10, 1990

Black crystals of $NH_4[Mo_2P_2O_{10}] \cdot H_2O$, (**1**), can be isolated by reacting MoO_3, Mo, $(NH_4)_2HPO_4$, H_3PO_4, and H_2O in a mole ratio of 3 : 1.1 : 2 : 4 : 120 for 16 hr at 360°C. The structure of phosphate (**1**) was determined and refined from single crystal data collected on a $35 \times 20 \times 10\ \mu m^3$ crystal at beamline X10A at NSLS, Brookhaven National Laboratory. Compound (**1**) is monoclinic, space group $P2_1/n$ with $a = 9.780(10)$, $b = 9.681(5)$, $c = 9.884(8)$ Å, $\beta = 102.17(8)°$, V = 915(1) Å^3 and $R(R_w) = 0.029(0.024)$ and contains MoO_6 octahedra and PO_4 tetrahedra. The structure is built up from Mo_4 oxo units that have two edge-sharing $Mo^{4+}O_6$ octahedra that contain Mo–Mo double bonds (2.453(2) Å), with the same two oxygens that bridge the Mo^{4+} also serving as a corner for two additional $Mo^{5+}O_6$ octahedra. The Mo_4 units are connected by phosphate groups into a 3-D array which generates several types of tunnel which are filled with NH_4^+ cations and H_2O. The material is isotypic with the mineral leucophosphite, $K[Fe_2(OH)(H_2O)(PO_4)_2] \cdot H_2O$. Water absorption isotherms show that (**1**) is microporous and has about 10–12 vol% internal void space that can be filled by water.

We have discovered several new mixed octahedral–tetrahedral frameworks in the molybdenum phosphate system that can be rendered microporous such as $(Me_4N)_{1.3}(H_3O)_{0.7}[Mo_4O_8(PO_4)_2] \cdot 2H_2O$ (*1*), $(NH_4)_3Mo_4P_3O_{16}$ (*2*), $Mo_8(H_2O)_6P_6O_{34}(OH)_2 \cdot 7H_2O$ (*3*), and $(CH_3)_2NH_2[Mo_2P_3O_{12}(OH)_2]$ (*4*). Here we describe the synthesis, structure, and sorption properties of $NH_4[Mo_2P_2O_{10}] \cdot H_2O$, (**1**), a new phosphate containing edge-sharing $Mo^{4+}O_6$ octahedra, with Mo–Mo double bonds, that are connected to corner sharing $Mo^{5+}O_6$ octahedra and an open framework containing 10–12 vol% void space as determined from water absorption isotherms. The material is isotypic with the mineral leucophosphite, $K[Fe_2(OH)(H_2O)(PO_4)_2] \cdot H_2O$ (*5*), as well as $GaPO_4 \cdot 2H_2O$ (*6*) and $NH_4[Al_2(OH)(H_2O)(PO_4)_2] \cdot H_2O$ (*7*).

When MoO_3, Mo, $(NH_4)_2HPO_4$, H_3PO_4, and H_2O are reacted in mole ratios of 3 : 1.1 : 2 : 4 : 120 for 16 hr at 360°C, $NH_4[Mo_2P_2O_{10}] \cdot H_2O$ is obtained in varying yields and is often contaminated by small amounts of an amorphous white solid. We performed over forty reactions using this stoichiometry (or various perturbations on the reaction conditions) but only obtained (**1**) about 15% of the time. These reactions are run on a 10^{-3} mol scale at very high pressures, the Mo starting materials are

* To whom correspondence should be addressed.

0022-4596/91 $3.00

insoluble solids, and there is no way to stir the reactions. When (**1**) did not form, either $(NH_4)_3Mo_4P_3O_{16}$ (*2*) or $NH_4[Mo_2P_3O_{12}(OH)_2]$ formed as essentially single phase products. These observations all suggest that the species that initially nucleates determines which product forms. When (**1**) did form, the sample also often contained small amounts of an amorphous white solid. We have observed that the heating rate during the initial phases of the reaction can have a large effect on the product obtained and are currently investigating this aspect.

Since the small size of the crystals available ($35 \times 20 \times 10\ \mu m^3$) precluded analysis by conventional X-ray sources, we determined the structure using beamline X10A at the National Synchrotron Light Source at Brookhaven National Laboratory. There have been few previous single-crystal synchrotron studies of such small-unit-cell structures (*8*) because of the inability to obtain high precision data. In the only previous full-structure determination from such data, residuals of $R(R_w) = 0.094(0.08)$ were obtained (*9*). Our results, which are on a crystal of comparable size and complexity, are of a much higher precision $R(R_w) = 0.029(0.024)$. This is due to the use of new experimental techniques, the main component of which is a new type of X-ray optics. Using a vertically defocused beam, we use three slits plus the small aperature presented by the sample diameter to define two, concident-path X-ray beams. Both of these beams are uniform in intensity over a ≈250 μm diameter. One of these beams is directed into a monitor for use in tracking temporal fluctuations of the beam. The second beam illuminates the sample. Because the slits defining this narrow beam are several meters apart, they produce a very narrow acceptance angle. This reduces the intensity variation that comes from spatial beam fluctuations of the sort that arise from small changes in the electron orbit. Reducing this effect is of critical importance because the intensity measurements for a structure determination are taken over several days of beamtime (*10*). Further details concerning the experimental techniques and structure determination are given in Table I. The atom coordinates are given in Table II.

TABLE I

CRYSTALLOGRAPHIC DETAILS FOR (**1**)

A. Experimental details	
Formula	$NH_4[Mo_2P_2O_{10}] \cdot H_2O$
Formual weight	449.87 g
Crystal dimensions	$35 \times 20 \times 10\ \mu m^3$
Crystal system	monoclinic
No. of reflections used for unit cell determination and refinement	13
Cell parameters	$a = 9.78(1)$ Å $b = 9.681(5)$ Å $c = 9.884\ (8)$ Å $\beta = 102.17°\ (8)$ $V = 915(1)$ Å^3
Space group	$P2_1/n$
Z value	4
D_{calc}	3.265 g cm^{-3}
F_{000}	860
$\mu_{(\lambda=0.915\ Å)}$	62.21 cm^{-1}
B. Intensity measurements	
Diffractometer	Huber 4-circle with vertical detector rotation
Monochromator	Double-Crystal Ge (111)
Radiation, NSLS X10A: 2.5 GeV, ≈125 mA	$\lambda = 0.915(2)$ Å
Energy resolution, $\Delta E/E$	10^{-4}
Detector aperture	Horizontal aperature = 12 mm Vertical aperature = 5mm
Crystal to detector distance	345 mm
Scan type	Omega, unequal step size
Points per scan	100
Scan width, deg	1.0
$2\theta_{max}$, deg	38.0
q range, $q = 2\pi \sin(\theta)/\lambda$	0.12 Å$^{-1} \leq q \leq$ 2.04 Å^{-1}
No. of reflections measured	Total (incl. 1 std. every 10 reflections) = 795 $I > 3\sigma_I = 662$ Unique, $I > 3\sigma_I = 581$
Corrections	Lorentz-polarization
C. Structure solution and refinement	
Structure solution	Direct methods (*16*)
Refinement	Full-matrix least-squares (*17*)
Function minimized	SUM[w*(/F$_O$/ − /F$_C$/)**2]
Least-squares weight	$1/\sigma_F^2$
Anomalous dispersion (Mo$K\alpha$ correction applied)	All nonhydrogen atoms
No. observations	581
No. variables	75
Reflection/parameter ratio	7.75
Residuals $R(R_w)$	0.029(0.024)

TABLE II

FRACTIONAL COORDINATES FOR (**1**)

A. Atom parameters

Atom	*x/a*	*y/b*	*z/c*	*U*(iso)[a]
Mo(1)	0.3968(1)	0.0350(1)	0.9132(1)	0.0037[b]
Mo(2)	0.1705(1)	0.1967(1)	0.4224(1)	0.0048
P(1)	0.8623(3)	0.1885(4)	0.2086(3)	0.0079(8)
P(2)	0.3430(3)	0.0165(4)	0.2093(3)	0.0099(9)
O(1)	0.9955(7)	0.5069(8)	0.2594(7)	0.012(2)
O(2)	0.7822(7)	0.0538(9)	0.2009(8)	0.012(2)
O(3)	0.7793(8)	0.6270(9)	0.7056(8)	0.012(2)
O(4)	0.5620(8)	0.1511(8)	−0.0028(8)	0.009(2)
O(5)	0.8146(7)	0.2858(8)	0.3081(8)	0.011(2)
O(6)	0.3058(7)	0.1016(9)	0.3261(8)	0.011(2)
O(7)	0.4793(8)	0.6595(8)	0.2475(8)	0.011(2)
O(8)	0.8679(8)	0.9362(9)	0.4875(8)	0.019(2)
O(9)	0.8429(8)	0.2501(8)	0.0598(8)	0.014(2)
O(10)	0.2028(7)	0.5882(8)	0.4328(8)	0.012(2)
O(11)	−0.012 (1)	0.163 (1)	0.740 (1)	0.067(4)
N(1)	0.116 (1)	0.321 (1)	0.982 (1)	0.045(4)

B. Anisotropic thermal parameters

Atom	*U*(11)[c]	*U*(22)	*U*(33)	*U*(23)	*U*(13)	*U*(12)
Mo(1)	0.0023(5)	0.0046(6)	0.0049(6)	0.0004(6)	−0.0009(4)	0.001(6)
Mo(2)	0.0029(5)	0.0069(7)	0.0057(6)	−0.0004(6)	−0.0005(4)	0.013(6)

[a] Coefficients of temperature factor T in A^2; $T = \exp(-8\pi^2\, U(\text{iso})\, (\sin\theta/\lambda)^2)$.
[b] Given in A^2; $Ueq = 1/3\ \Sigma_i\ \Sigma_j\ U_{ij}\, a_i^* a_j^* a_i a_j$.
[c] Coefficients of temperature factor T in $Å^2$; $T = \exp(-2\pi^2\ \Sigma_i\ \Sigma_j\ U_{ij} h_i h_j\, a_i a_j)$.

The structure (see Table III for bond lengths and angles) of (**1**) is best described in terms of the Mo_4 building blocks, (**A**), which resemble the Mo_4 unit (**B**), found in $Mo_8(H_2O)_6P_6O_{34}(OH)_2 \cdot 7H_2O$ (*3*), (**2**). Both centrosymmetric clusters are shown in Fig. 1 for comparison. Both have a central pair of edge-sharing (via O(4)) MoO_6 octahedra: these Mo atoms in (**A**) are connected by a Mo–Mo double bond (*11*) of 2.453(2) Å and have a calculated (*12*) oxidation state of 3.7+ based on the observed Mo–O bond lengths, while the analogous pair of octahedra in (**B**) contain Mo^{5+} and a Mo–Mo single bond of 2.63 Å (*3*). In both (**A**) and (**B**) there are two additional Mo^{5+} containing octahedra, one corner of which is also O(4), making those oxygens three coordinate. The two central Mo^{5+} in (**B**) have disordered molybdenyl/water oxygen atoms over the four O sites perpendicular to the Mo_4 plane whereas in (**A**) the corresponding positions on the Mo^{4+} dimer are occupied by the oxygens of a bridging PO_4 tetrahedra.

These Mo_4 units are bridged together into a 3-D structure by PO_4 groups which generates an intersecting array of tunnels running through the structure. The tunnels are filled with equal numbers of NH_4^+ (at 1/2, 1/2, 0) and H_2O (at 0, 1/2, 0). A projection of the

TABLE IIIA
BOND LENGTHS

Atom–atom		Distance (Å)
Mo(1)		
	–Mo(1)	2.453(2)
	–O(1)	2.006(7)
	–O(2)	2.060(7)
	–O(4)	1.999(7)
	–O(4)	2.010(7)
	–O(5)	2.094(8)
	–O(10)	2.039(8)
Mo(2)		
	–O(3)	2.241(8)
	–O(4)	2.044(8)
	–O(6)	2.009(8)
	–O(7)	2.015(8)
	–O(8)	1.652(8)
	–O(9)	1.997(8)
P(1)		
	–O(2)	1.515(9)
	–O(5)	1.505(9)
	–O(7)	1.543(9)
	–O(9)	1.560(9)
P(2)		
	–O(1)	1.547(8)
	–O(3)	1.520(9)
	–O(6)	1.523(9)
	–O(10)	1.546(9)

TABLE IIIB
O–*M*–O ANGLES

Mo(1) octahedron	
O(1)–Mo(1)–O(2)	89.43(31)
O(1)–Mo(1)–O(4)	87.28(31)
O(1)–Mo(1)–O(4)	93.97(32)
O(1)–Mo(1)–O(5)	89.27(30)
O(1)–Mo(1)–O(10)	177.02(34)
O(2)–Mo(1)–O(4)	168.85(33)
O(2)–Mo(1)–O(4)	86.31(31)
O(2)–Mo(1)–O(5)	83.17(30)
O(2)–Mo(1)–O(10)	91.69(29)
O(4)–Mo(1)–O(4)	104.54(26)
O(4)–Mo(1)–O(5)	86.13(30)
O(4)–Mo(1)–O(10)	91.10(31)
O(4)–Mo(1)–O(5)	168.96(28)
O(4)–Mo(1)–O(10)	88.86(33)
O(5)–Mo(1)–O(10)	88.12(31)
Mo(2) octahedron	
O(3)–Mo(2)–O(4)	81.21(30)
O(3)–Mo(2)–O(6)	80.60(30)
O(3)–Mo(2)–O(7)	82.69(30)
O(3)–Mo(2)–O(8)	178.26(36)
O(3)–Mo(2)–O(9)	86.18(30)
O(4)–Mo(2)–O(6)	161.11(32)
O(4)–Mo(2)–O(7)	95.07(30)
O(4)–Mo(2)–O(8)	99.92(35)
O(4)–Mo(2)–O(9)	89.79(31)
O(6)–Mo(2)–O(7)	87.66(31)
O(6)–Mo(2)–O(8)	98.38(37)
O(6)–Mo(2)–O(9)	83.94(31)
O(7)–Mo(2)–O(8)	95.87(36)
O(7)–Mo(2)–O(9)	167.03(32)
O(8)–Mo(2)–O(9)	95.12(35)
P(1) tetrahedron	
O(2)–P(1)–O(5)	110.03(43)
O(2)–P(1)–O(7)	109.58(45)
O(2)–P(1)–O(9)	108.81(45)
O(5)–P(1)–O(7)	111.18(44)
O(5)–P(1)–O(9)	112.56(45)
O(7)–P(1)–O(9)	104.51(44)
P(2) tetrahedron	
O(1)–P(2)–O(3)	110.23(45)
O(1)–P(2)–O(6)	106.13(41)
O(1)–P(2)–O(10)	107.28(42)
O(3)–P(2)–O(6)	110.49(44)
O(3)–P(2)–O(10)	110.47(44)
O(6)–P(2)–O(10)	112.11(44)

structure down [010] is shown in Figs. 2a and 2b. To visualize the 3-D connectivity of the framework of (**1**), one can consider the structure to consist of layers lying in the (101) plane. One can isolate these layers from the structure via excission of the O(6) atoms which lie near the (202) plane (Figs. 2a and 2b). One such layer is shown in Fig. 2c and 2d, which is a projection down [101] and shows the interlayer connectivity of tetramer (**A**) into sheets by the phosphate groups.

Thermogravimetric analysis (TGA) shows that at a heating rate of 5°C · min^{-1} in He, the sample starts losing water at $T > 30$°C and there is a weight loss of 3% completed at ca. 100°C (calculated for the loss of one H_2O, 4%). Continued heating gives a gradual 3.5% weight loss in the

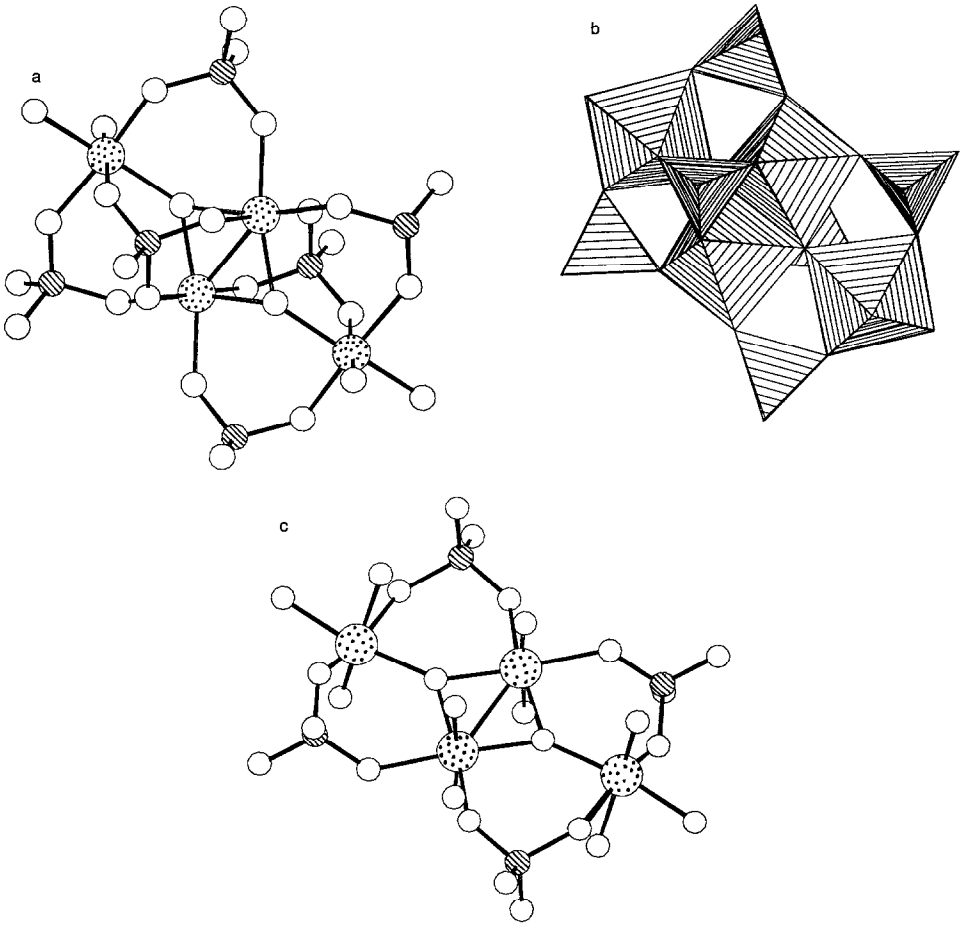

FIG. 1. The Mo_4 tetramer (**A**) found in (**1**) shown as both (a) ball-and-stick (*14*) and (b) polyhedral representations (*15*); (c) the similar Mo_4 tetramer (**B**) found in $Mo_8(H_2O)_6P_6O_{34}(OH)_2 \cdot 7H_2O$ (*3*) (see text). The Mo are stippled. Note the additional phosphate groups in tetramer (**A**).

150–300° range from NH_3 removal (calculated value = 4%). IR spectra show that the absorption due to the NH_4^+ is gone after the heat treatment. Samples of (**1**) are microporous as demonstrated by the Type I absorption isotherm (*13*) shown in Fig. 3. Although the absorption is totally reversible, and both the H_2O and the NH_4^+ are removed during the heating/degas cycle according to the TGA data, the amount reabsorbed at 20°C corresponds to filling only about half of the space that was occupied by the H_2O and the NH_4^+. The width of the peaks in the powder X-ray diffraction pattern of (**1**) are essentially unchanged after heating to 500°C under He, suggesting little loss of order in the lattice; however, absorption isotherms after heating to 550°C show the sample only sorbs <1 wt% H_2O and most of it adsorbs to the surface. This may be due to the tunnels being partially blocked by dehydroxylation (there is a weight loss observed in the TGA at ca. 410°C, typical of water loss in an oxide from dehydroxylation) from the hydroxyl groups generated from the proton left behind when the NH_4^+ decomposed to NH_3

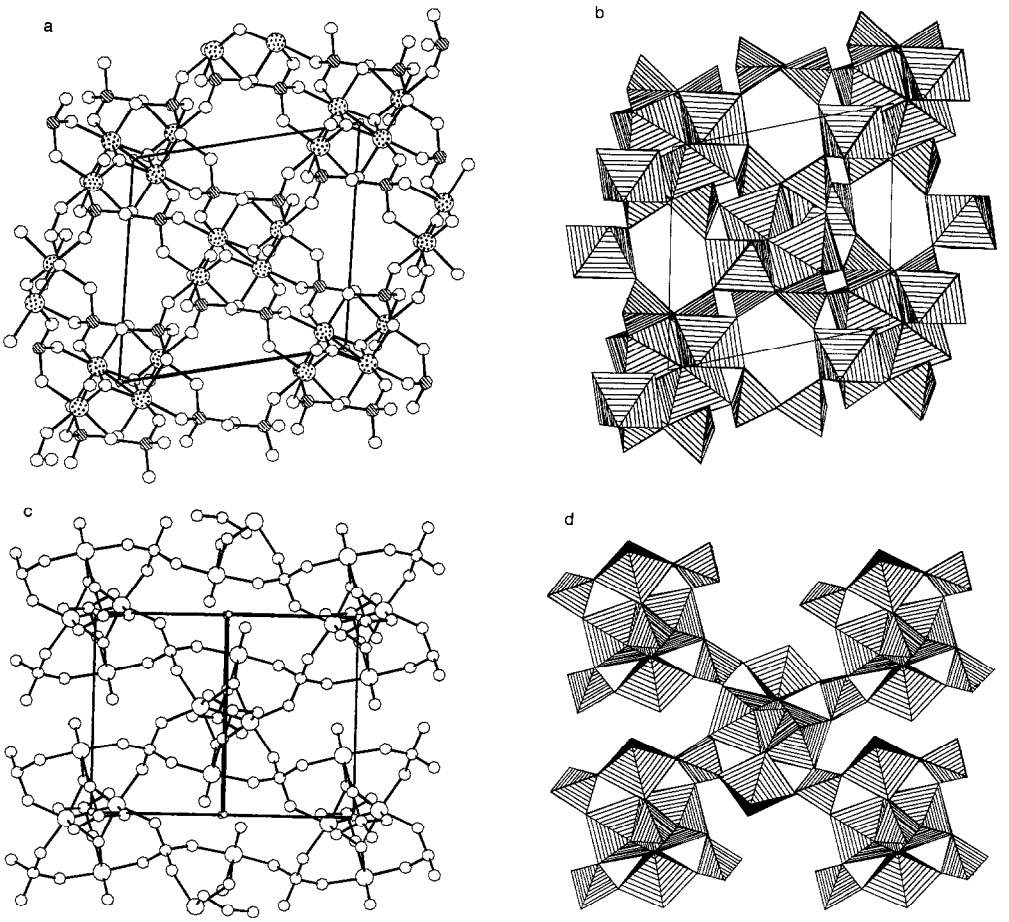

FIG. 2. Ball-and-stick and polyhedral projections of the unit cell contents of (**1**) down [010] (a and b) down [101] (c and d). The water and NH_4^+ molecules in the tunnels are not shown.

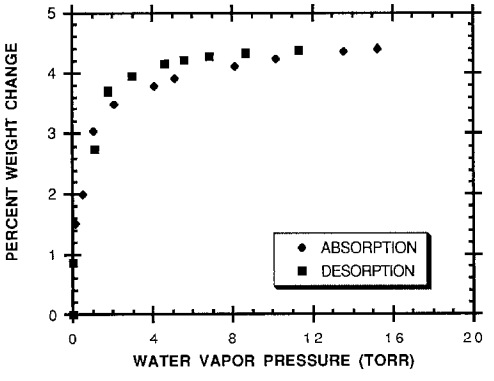

FIG. 3. Water absorption isotherm for degassed (**1**) at 20°C demonstrating the absorption of water into the micropores (degas conditions: 200°C for 4 hr at 10^{-3} Torr).

and H^+. The other isotypes discussed above have much less thermal stability probably due to the presence of terminal H_2O ligands and hydroxy groups whereas (**1**) has terminal molybdenyl and oxo groups in the corresponding parts of the structure.

The tetrameric Mo_4 unit, and its associated PO_4 tetrahedra, is topologically identical to the hydrated hydroxy ferric phosphate unit found in the mineral leucophosphite (*5*). In this mineral, which is usually pale green and has an Fe–Fe distance of 3.11 Å, there appears to be little metal–metal interaction, unlike the 2.45 Å metal–metal double bond contact found in (**1**).

We are currently examining other syn-

thetic routes to (**1**) in attempts to improve the yield, phase purity, and reproducibility.

Acknowledgments

We are grateful to Dr. Paul B. Moore, University of Chicago, for alerting us to his structure determination of leucophosphite and for many stimulating discussions. We thank the U.S. Department of Energy which operates the National Synchrotron Light Source at Brookhaven National Laboratory.

References

1. R. C. HAUSHALTER, K. G. STROHMAIER, AND F. W. LAI, *Science* **246,** 1289 (1989).
2. R. HAUSHALTER, L.MUNDI, AND H. E. KING, JR., *J. Solid State Chem.*, in press.
3. R. HAUSHALTER, L. MUNDI, D. GOSHORN, AND K. STROHMAIER, *J. Amer. Chem. Soc.* **112,** 8183 (1990).
4. R. HAUSHALTER, L. MUNDI, AND K. STROHMAIER, *Inorg. Chem.*, in press.
5. P. B. MOORE, *Amer. Mineral.* **57,** 397 (1972).
6. R. C. L. MOONEY-SLATER, *Acta Crystallogr.* **20,** 526 (1966).
7. J. J. PLUTH, J. V. SMITH, J. M., BENNETT, AND J. P. COHEN, *Acta Crystallogr. Sect. C* **40,** 2008 (1984).
8. R. BACKMANN, H. KOHLER, H. SCHULZ, AND H. WEBER, *Acta Crystallogr. Sect. A* **41,** 35 (1985); F. S. Nielsen, P. Lee, and P. Coppens, *Acta Crystallogr. Sect. B* **42,** 359 (1986); P. Süsse, M. Steins, and V. Kupcik, *Zeit. Kristallogr.* **184,** 1988 (1988).
9. S. A. ANDREWS, M. Z. PAPIZ, R. MCMEEKING, A. J. BLAKE, B. M. ŁOWE, K. R. FRANKLIN, J. R. HELLIWELL, AND M. M. HARDING, *Acta Crystallogr. Sect. B* **44,** 73 (1988).
10. The experimental details of the synchrotron crystallography will be published elsewhere; H. E. King, Jr., R. Haushalter, unpublished results, 1990.
11. M. H. CHISHOLM, *Polyhedron,* **2,** 681 (1982) and references therein.
12. I. D. BROWN, AND K. K. WU, *Acta Crystallogr. Sect. B* **32,** 1957 (1976); W. H. Zachariasen, *J.Less-Common Metals* **62,** 17 (1978).
13. D. M. RUTHVEN, "Principles of Adsorption and Adsorption Processes," p. 49 Wiley, New York, (1984).
14. CHEM-X, designed and distributed by Chemical Design, Ltd., Mahwah, NJ.
15. STRUPLO-84, R. X. Fischer, *J. Appl. Crystallogr.* **18,** 258 (1985).
16. Structure Determination Package, Enraf-Nonius Co., Delft, Holland.
17. Crystals, Chemical Crystallography Laboratory, Oxford University, Oxford, England.